FUSING 3 AND 7 TESLA HCP DATASETS FOR IMPROVED BRAIN CONNECTIVITY ANALYSIS

Stamatios N Sotiropoulos[1], Saad Jbabdi[1], An T Vu[2], Jesper L Andersson[1], Steen Moeller[2], Christophe Lenglet[2], Essa Yacoub[2], Kamil Ugurbil[2], and Timothy Behrens[1]
[1]*FMRIB Centre, University of Oxford, Oxford, United Kingdom,* [2]*Center for Magnetic Resonance Research, University of Minnesota, Minneapolis, MN, United States*

Target Audience: This work will be of interest to scientists studying fibre orientation and brain connectivity modeling using 3T and 7T diffusion MRI.

Purpose: The trade-off between signal to noise ratio (SNR) and spatial specificity governs the choice of spatial resolution in MRI. In diffusion MRI (dMRI) the trade-off is further complicated by the choice of angular diffusion contrast. Images of lower resolution have less spatial specificity but higher signal to noise ratio (SNR), which can be further invested into higher angular contrast, important for resolving complex fibre patterns [1]. Considering these trade-offs, the Human Connectome Project (HCP) acquires 3 tesla (3T) data of very high quality [2], both in terms of spatial and angular resolution [3]. However, amongst the efforts to develop transferable technology and push the limits of in-vivo scans, a subset of the HCP subjects are also scanned at 7 tesla (7T). Due to differences in the signal behaviour at different field strengths (higher baseline SNR and shorter T2 at 7T) and in the underlying scanner hardware (max gradient strength of 100 mT/m at 3T and 70 mT/m at 7T) [2], the HCP 3T and 7T data of the same subject have different, but complementary features, which we illustrate. Then, we present a framework for fusing both datasets into a single fibre orientation estimation analysis, which allows us to get the benefits of both worlds and improve brain connectivity estimation.

Methods: The HCP 3T data are comprised of 1.25mm^3 voxels (nominal resolution) acquired at 3 shells (b=1000, 2000 and 3000 s/mm^2) with 90 directions per shell acquired twice [3]. A multiband (MB) acceleration factor of 3 is used [4] without any in-plane parallel imaging. The HCP 7T data are comprised of 1.05 mm^3 voxels acquired at 2 shells (b=1000 and 2000 s/mm^2) with 65 directions per shell acquired twice with a MB factor of 2 and in-plane GRAPPA factor of 3 [5]. Despite the seemingly small difference in nominal resolution (which still results to a 7T voxel volume being 59% of the 3T), the 7T data are closer to their nominal resolution, due to a shorter echo train (41ms vs 85ms at 3T) and smaller PSF blurring along the phase-encoding direction (see in Fig. 1 the difference in the FA maps crispness). Indeed, when calculating "true" voxel volumes using FWHMs taking into account the PSF in each case, the 7T voxel volume is ~41% of the 3T. On the other hand, the 3T data contain more angular information for resolving fibre crossings.

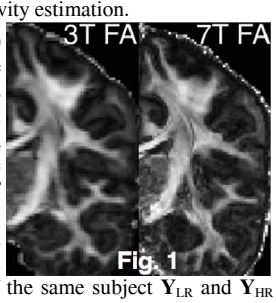

Spherical Deconvolution by Data Fusion: A parametric approach has been developed for performing neighbourhood-wise spherical deconvolution by fusing data acquired at different spatial resolutions. The underlying generative model (RubiX) has been presented in [6]. Here we extend it to account for the multi-shell nature of the datasets. Briefly, let's assume the generic case of two datasets of the same subject $\mathbf{Y}_{LR}$ and $\mathbf{Y}_{HR}$ acquired at different resolutions, low (LR) and high (HR) respectively. After aligning the data, we are looking to estimate a set of parameters ω_{HR} that describe the fibre orientation distribution functions (fODFs) at the HR grid. We can use a convolution model to get a prediction of $\mathbf{Y}_{HR}$ given the parameters. We can then use a partial volume model on the signal predictions of the HR voxels $\{\mathbf{B_k}\}$, intersecting a LR voxel $\mathbf{A}$, to predict the LR signal at $\mathbf{A}$. Using this hierarchical framework, we can invert the model given both $\mathbf{Y}_{LR}$ & $\mathbf{Y}_{HR}$ and estimate ω_{HR}. We use Bayesian inference to perform this inversion and use priors that: a) allow on-line fibre complexity selection by considering both datasets and b) regularise spatially the orientation solutions (see [6] for details on the priors). The HR model uses a sum of delta functions for the fODF and a gamma distribution of diffusivities to perform deconvolution using multi-shell data [7]. The LR model uses a weighted summation of HR signal attenuations [6]. The framework effectively allows orientations deconvolved at the LR (i.e. more robust due to higher SNR/angular information) to be used as constraints on the deconvolution of HR orientations (i.e. higher spatial specifity, but more "noisy"), while importantly estimating these constraints as well from the data. This fusion results to more accurate and precise deconvolution at the HR, compared to deconvolution performed at the HR data alone (when matched for acquisition time) with a minimal loss of spatial specificity [6].

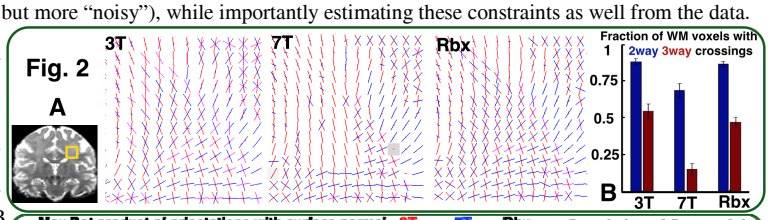

Results and Discussion: Fig. 2 shows an example where a desirable feature from the 3T data (i.e. high support for fibre complexity) is preserved after data fusion. Fig. 2A shows orientations estimated at the centrum semiovale using the 3T and 7T data alone (i.e. voxel-wise spherical deconvolution [7]) and after fusing the data using RubiX (i.e. use 3T as "LR" and 7T as "HR"). Fig. 2B shows the amount of 2- & 3-way crossings estimated in white matter using the three approaches. Notice that the RubiX estimates are estimated at HR and have spatial specificity representative of the HR grid [6]. These results illustrate that the 7T data alone do not support as high fibre complexity as the 3T. However, with data fusion we can achieve similar complexity levels to the 3T, while being at higher resolution.

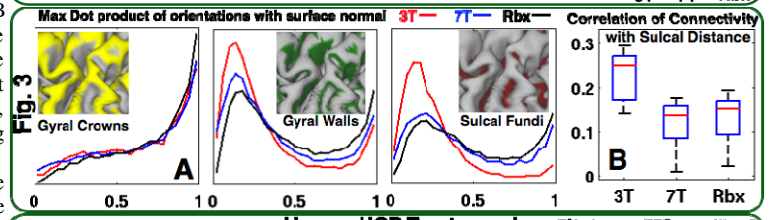

Fig. 3 shows an example where a desirable feature from the 7T data (i.e. more spreading of orientations towards the cortex) is preserved after data fusion. Due to higher spatial resolution, 7T data allow more orientations that are perpendicular to the WM/GM boundary surface to be estimated compared to the 3T. This is illustrated in Fig. 3A that shows histograms of the dot product of estimated fibre orientations with the surface normal at different areas of the WM/GM boundary surface (gyral crowns, gyral walls and sulcal fundi). Particularly for the walls and the sulcal fundi, the majority of 3T fibre orientations are parallel to the surface. With 7T there are less parallel and more perpendicular orientations to the surface and that trend is preserved (even slightly improved) with RubiX. The result of the 3T orientation pattern is an anatomically-inaccurate bias of tractography connections towards the gyral crowns [8]. Fig. 3B shows boxplots that represent the correlation of the total (tractography-estimated) connectivity per WM/GM boundary surface vertex (~60,000 vertices in total) with the sulcal distance (i.e. distance of this vertex from the nearest sulcal fundus), across 5 subjects. Gyral crowns tend to have higher estimated connectivity. Due to the different orientation pattern resolved near the cortex, 7T data reduce this bias and RubiX successfully preserves that.

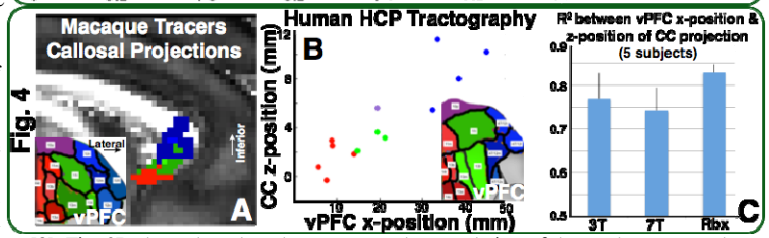

Fig. 4 shows the ability to recover connection organisation rules using tractography and comparing results to ground-truth chemical tracing. Chemical tracers suggest that callosal projections from subregions of the ventral PreFrontal Cortex (vPFC) adhere to the following rule: The more lateral the vPFC subregion is, the more superior its callocal projections are within the midsagittal corpus callosum (Fig. 4A) [9]. Very high quality post-mortem macaque dMRI data can replicate such a strong correlation through tractography (R^2=0.94) [9]. As shown in Fig. 4B, the HCP data allow this rule to be recovered across individual subjects. The RubiX framework achieves however the largest and more reproducible across subjects correlation (Fig. 4C) ($\langle R^2 \rangle$=0.83 for RubiX vs $\langle R^2 \rangle$=0.76, 0.74 for 3T, 7T respectively).

Conclusion: We have presented a framework for fusing dMRI data acquired at different scanners/sequences with complementary spatial/angular features. The approach, although applied specifically to HCP data here, is a more generic framework that illustrates the value of performing neighbourhood-wise spherical deconvolution for improving robustness and precision in brain connectivity analysis.

References: **1**. Tournier et al, NeuroImage 23:1176-85, 2004. **2**. Ugurbil et al, NeuroImage 80:80-104, 2013. **3**. Sotiropoulos et al, NeuroImage 80:125-43, 2013. **4**. Moeller et al, MRM 63 1144-53, 2010. **5**. Vu et al, ISMRM, 1000, 2014. **6**. Sotiropoulos et al, IEEE TMI 32: 969-82, 2013. **7**. Jbabdi et al, MRM 68:1846-55, 2012. **8**. Van Essen et al, Diffusion MRI (2nd Edition), Elsevier, 337-358, 2013. **9**. Jbabdi et al, J. Neuroscience 33:3190-3201, 2013.

Acknowledgement: We would like to ackowledge funding from the NIH through the Human Connectome Project (1U54MH091657-01) and EPSRC (EP/L023067/1).